Oak timber cross-cutting based on fiber orientation scanning and mechanical modelling to ensure finger-joints strength

SOH MBOU Delin[1*], BESSEAU Benoit[2], POT Guillaume[1], VIGUIER Joffrey[1], MARCON Bertrand[1], MILHE Louis[1], LANVIN Jean-Denis[3], REULING Didier[3]

[1] Arts et Metiers Institute of Technology, LaBoMaP, UBFC, HESAM Université, F-71250 Cluny, France.
[2] Ducerf Groupe, Le Bourg, 71120 Vendenesse-lès-Charolles, France.
[3] FCBA, Allée de Boutaut BP227, 33028 Bordeaux, France.

E-mail: delin.soh_mbou@ensam.eu; benoit.besseau@ducerf.com; guillaume.pot@ensam.eu; joffrey.Viguier@ensam.eu; bertrand.marcon@ensam.eu; louis.milhe@ensam.eu; jean-denis.lanvin@fcba.fr; didier.reuling@fcba.fr

Keywords: cross-cutting, finger-joint, glued laminated timber, knot, slope of grain, oak

ABSTRACT

The mechanical properties of wood depend on its characteristics at different scales, in particular its knots and the orientation of its fibers. As wood is a highly anisotropic material, its strength and elastic properties are much better in the longitudinal direction of the fibers than in the perpendicular directions, so the orientation of the fibers is an extremely important parameter. Finger-jointing is a technique for joining sawn timbers into large panels for structural use, such as finger-jointed panels (GLT) and laminated timbers (CLT). In this study, the tensile strength of oak sawn timbers was modelled by considering the local fiber orientation obtained by using laser diffusion patterns onto the timber faces. Strength thresholds were established to ensure an equivalent mechanical performance to T11 tensile strength class, with the possibility of cross-sectional splitting if required. In addition, the tensile strength of the finger-joints was determined in accordance with (NF EN 14080 2013). Lamellas were assembled, glued and subjected to tensile tests, and the method was found to be satisfactory in terms of characteristic strength of the finger joints.

INTRODUCTION

Finger-jointed lamellas are used in the manufacture of large glued laminated timber (GLT) beams or cross laminated timber (CLT) panels. The aim of finger-jointing is to produce long timber elements while removing the weakest parts of the wood by cross-cutting. According to (NF EN 14080 2013), t finger joint strength is ensured by checking it's distance to a knot relatively to its diameter, d: "the grain at the cross-cut shall be approximately parallel to the axis of the board. The distance between the edge of a knot and the cross cut shall be at least 1.5 d. The grain deviation needs not to be checked if the distance is 3 d". It is important to note that the (NF EN 14080 2013) standard applies for GLT made of coniferous species or poplar, no standard for CLT nor GLT exists yet. For GLT made of hardwood, a standard is being prepared, but an European assessment document already exists (EAD 130320-00-0304 2018), using the exact same rule to ensure finger-joint strength. However, hardwood anatomy is very different from that of coniferous and thus knot limits are much more difficult to define on hardwoods. In addition, significant fiber deviation can appear whereas no knots are really visible in the considered board. Fiber deviation is very difficult to observe visually, as an operator is reduced to guessing based on the shapes drawn by growth rings, the parenchyma orientation (for the species for which they are visible by naked eye), and so on. As a result, this rule looks very difficult to apply and can be more restrictive for hardwoods than softwoods, because knots are often larger (requiring to remove more material when it comes to produce GLT or CLT applying the existing standard restrictions).

Fiber orientation can be measured by an industrial laser scanning machine. Due to the anisotropic scattering properties of wood, the resulting image of a laser spot on the wood surface takes the form of an ellipse. The major axis of this ellipse is aligned in the direction of the fiber orientation, a phenomenon known in the literature as the "tracheid effect" . This name derives from the first observations on softwoods (Nyström 2003) (Simonaho et al. 2002) and (Simonaho and Silvennoinen 2004), which is

based on the anisotropic scattering of concentrated laser light projected onto the wood surface (Daval et al. 2015; Purba et al. 2020) . (Olsson et al. 2019) and (Besseau 2021) suggested using fiber orientation measured from such scanners to ensure the finger-joint strength rather than knot diameter (*d*) or distance to knot. Both authors offering promising prospects for reducing material waste and improving the reliability of finger-jointed lamellas. (Olsson et al. 2019) defined a threshold of 8° to determine quantitatively when fibers are "approximately parallel to the axis of the board" as it is stated in (NF EN 14080 2013) standard. They found out that wasted material when cross-cutting Norway spruce can be decreased from 7.4% to 4% when applying a rule based on a minimum distance of 1.5 times *d* from the knot and a fiber deviation below 8°. However, the results were not validated by actual mechanical tests on the finger-joint. (Besseau 2021) dealt with French oak hardwood species measuring of fiber deviation on the timbers faces with a scanner around various finger-jointed samples, and then performed bending tests on them. This approach is similar to that of machine timber strength grading (EN 14081-2+A1 2022), like a non-destructive testing of finger-jointed lamellas. Thereby, the results were similar than in timber strength grading enabling to introduce an Indicating Properties (IP) that can be used as a threshold to exclude too weak finger joints. However, the objective of an industrial process would be to define cross-cutting positions on the basis of a threshold before performing the finger jointing, and not having to exclude lamellas with weak finger-joints.

The objective of the present work is to define a method based solely on fiber orientation scanning data to perform the cross-cutting operations, ensuring the resistance of both the finger-joints and the short-length wood elements between these joints, in the case of oak timber lamellas. Eventually, this approach aims to propose a standardized machine method to ensure finger-joints strength that could be more consistent and efficient than the current visual method, especially in the case of hardwood.

For this purpose, a method to compute the averaged 3D fiber orientation across the cross-section was firstly defined. This data was used to define an IP of tensile strength based on more than 900 tensile tests of oak sawn timber. Then, cross-cutting operations were performed, relying on this IP to define the appropriate cross-cutting positions which ensure both plain wood and finger-jointed strength of a given lamella strength class. The cross-cut elements were finger-jointed together, and finally tensile tests were performed to verify the method.

MATERIALS AND METHODS

Lists of main abbreviations used in this article

Table 1: Lists of main abbreviations used

Symbol / Abbreviation	Description
MoE	Modulus of elasticity (MPa)
E_0	Modulus of elasticity in the longitudinal direction of fibers (MPa)
E_{90}	Modulus of elasticity in the transversal direction of fibers (MPa), the material being considered as transversely isotropic (no difference between the radial and tangential material directions)
G_{LTrans}	Shear modulus in transversal-longitudinal plane of fibers (MPa)
ν_{LTrans}	Poisson's ratio characterizing the transversal strains in relation to longitudinal one
γ_{xyz}	Spatial orientation angle of a fiber element (°)
$f_{t,0,k}$	Axial tensile strength for wood (MPa)
$f_{t,j,k}$	Axial tensile strength for finger joints (MPa)
d	Knot diameter (mm)

Calculation of fiber orientation in sawn timber

So far, the fiber orientation has primarily been considered in the plane, that of the surface on which elliptical light scattering of the laser dots is captured. This means that the measured angle is actually the projection of the actual fiber orientation within the wood material.

As proposed in (Besseau 2021), in the present article and parallelly in (Pot et al. 2024), a 3D angle was calculated by interpolating the planar angles measured on the orthogonal large and narrow faces of a wood plank. Figure 1 illustrates the configuration in the coordinate system ($\vec{x}$,$\vec{y}$,$\vec{z}$) of a volume element of wood with the average fiber direction represented by the vector ($\vec{u}_{\text{Fiber}}$). The projection of this vector

onto the ($\vec{x}$,$\vec{y}$) plane is denoted by ($\vec{u}_{xy}$) while the projection onto the ($\vec{x}$,$\vec{z}$) plane is noted as ($\vec{v}_{xz}$). The three-dimensional orientation of a fiber element is determined by the angle γ_{xyz} between ($\vec{u}_{Fiber}$) and the normal vector ($\vec{n}$) which coincides with the ($\vec{x}$) direction, *i.e.* the axial direction of the plank. Coordinates b and c can be expressed in terms of a using Eq. 1 and 2.

$$b = a \times \tan(\alpha_{xy}) \quad (1)$$

$$c = a \times \tan(\beta_{xz}) \quad (2)$$

The 3D angle γ_{xyz} being expressed as a combination of α_{xy} and β_{xz} angles:

$$\vec{u}_{Fibre} \cdot \vec{x} = \|\vec{u}_{Fibre}\| \times \|\vec{x}\| \times \cos(\gamma_{xyz}) \quad (3)$$

$$\cos(\gamma_{xyz}) = \frac{\vec{u}_{Fibre} \cdot \vec{x}}{\|\vec{u}_{Fibre}\| \times \|\vec{x}\|} = \frac{a}{\sqrt{a^2 + b^2 + c^2}} \quad (4)$$

$$\gamma_{xyz} = arc\left(\frac{1}{\sqrt{1 + tan^2(\alpha_{xy}) + tan^2(\beta_{xz})}}\right) \quad (5)$$

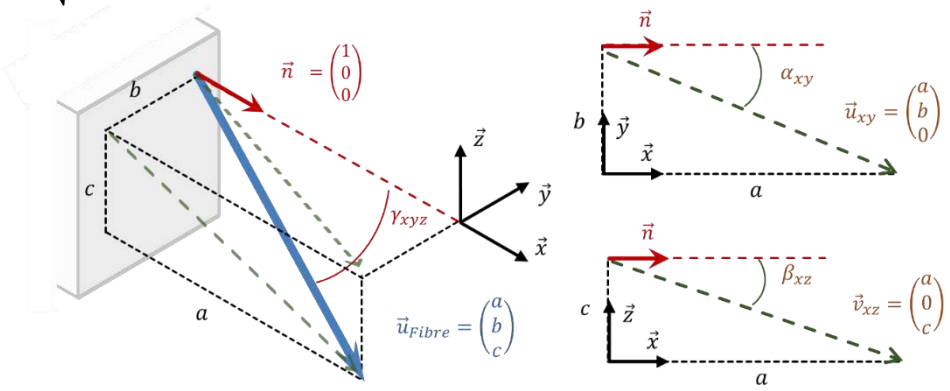

Figure 1 : Setting a fiber element in space (Besseau 2021)

When considering a plank of rectangular cross-section, fiber orientation data on the four scanned faces provides what corresponds to the surface angles α_{xy} and β_{xz} for large and narrow faces, respectively. These planar angle measurements on the plank envelope are insufficient to calculate precisely angles γ_{xyz} within the timber volume. An interpolation method is proposed to overcome this difficulty, The missing values are located in the cross-sectional area of the plank, which is subdivided into $1 \times 1 \times 1$ mm^3 cubes. For fibers beneath the two larger faces of a wood plank, the α_{xy} angles are directly derived from laser measurements, while the diving angles β_{xz} are only known at the ends. For fibers beneath the edges, the situation is reversed: the β_{xz} angles are known, but not the α_{xy} angles except at the ends. The missing components of angles α_{xy} et β_{xz} angles were respectively obtained through linear interpolation in thickness and width.

<u>Local MoE based on fibers orientation</u>

In practice, in the absence of an automatic and precise method for differentiating the radial direction from the tangential direction, a transverse isotropic model was preferred. The material properties were therefore defined as follows: E_0, the modulus of elasticity in the longitudinal direction of the fibers, was set at the 95th percentile of the experimental results of the study (Pot et al. 2024) used as a reference for the local modulus of elasticity in tension, i.e., 14620 MPa. The choice of the value of E_L is of little importance since relative comparisons were made; however, choosing such a value makes the absolute results of the modelled local moduli of elasticity consistent with the measured local moduli of elasticity, which is more practical. The value of E_0 influenced other material properties such as transverse modulus and shear modulus. Indeed, E_{90}, the modulus of elasticity in the direction orthogonal to the local fiber direction in this transverse isotropic model was calculated as the average of the orthotropic ratios E_R/E_L and E_T/E_L from (Kretschmann 2010) and regularized by the actual 95th percentile longitudinal stiffness of the set (E_0, from (Pot et al. 2024)). G_{LTrans} the shear modulus in the transverse isotropic plane was

similarly calculated as the average of the orthotropic ratios G_{LT}/E_L and G_{LR}/E_L from (Kretschmann 2010), and multiplied as before by E_0. Finally, ν_{LTrans} the Poisson's ratio in the transverse isotropic model, was taken equal to the average of the orthotropic Poisson's ratios ν_{LT} and ν_{LR} from (Kretschmann 2010), which is 0.4.

Table 2: Orthotropic mechanical properties of oak according to (Kretschmann 2010) and the corresponding simplified isotropic transverse mechanical properties introduced for the present research.

E_L	E_R	E_T	G_{LR}	G_{LT}	ν_{LR}	ν_{LT}
(MPa)	(MPa)	(MPa)	(MPa)	(MPa)		
14000	2280	1010	1200	1100	0.37	0.43
E_0	E_{90}		G_{LTrans}		ν_{LTrans}	
(MPa)	(MPa)		(MPa)			
14620	1718		1201		0.4	

These parameters can be arranged in the compliance matrix [S] of Eq. 1 from the local material system (L, Trans):

$$[S] = \begin{bmatrix} \frac{1}{E_0} & -\frac{\nu_{TransL}}{E_{90}} & 0 \\ -\frac{\nu_{LTrans}}{E_0} & \frac{1}{E_{90}} & 0 \\ 0 & 0 & \frac{1}{G_{LTrans}} \end{bmatrix} \quad (6)$$

For each element of the grid of interpolated angles γ_{xyz}, the material compliance matrix $[S]$ was rotated according to γ_{xyz}, by application of Eq. 7 using the basis changing transfer matrix (here being a rotation matrix $[T_\gamma]$ [OBJ],$\vec{x}$to obtain the local compliance matrix in the specimen system of axes ($\vec{y}$,$\vec{z}$,[S']) (x, y, z) for each (x, y, z) location:

$$[S'] = [T_\gamma^{-1}]\,[S]\,[T_\gamma] = \begin{bmatrix} S'_{11} & S'_{12} & S'_{16} \\ S'_{12} & S'_{22} & S'_{26} \\ S'_{16} & S'_{26} & S'_{66} \end{bmatrix} \quad (7)$$

$$\text{with } [T_\gamma] = \begin{bmatrix} Cos^2(\gamma_{xy}) & Sin^2(\gamma_{xy}) & 2 \times Cos(\gamma_{xy}) \times Sin(\gamma_{xy}) \\ Sin^2(\gamma_{xy}) & Cos^2(\gamma_{xy}) & -2 \times Cos(\gamma_{xy}) Sin(\gamma_{xy}) \\ -Cos(\gamma_{xy}) \times Sin(\gamma_{xy}) & Cos(\gamma_{xy}) \times Sin(\gamma_{xy}) & Cos^2(\gamma_{xy}) - Sin^2(\gamma_{xy}) \end{bmatrix}$$

the transfer matrix, from the local fiber coordinate system to the global specimen coordinate system, dependent on the fiber orientation γ_{xyz} obtained locally (abbreviated γ in the following). This gives E_x, the MoE in the main, lengthwise direction of the specimen ($\vec{x}$), as the inverse of the first coefficient of the compliance matrix [S']:

$$E_x(x, y, z) = \frac{1}{S'_{11}} = \frac{1}{\frac{1}{E_{90}}\sin^4(\gamma) + \frac{1}{E_0}cos^4(\gamma) + \left(\frac{1}{G_{LTrans}} - 2\frac{\nu_{LTrans}}{E_0}\right)\sin^2(\gamma)\,cos^2(\gamma)} \quad (8)$$

The average longitudinal stiffness of the plank was calculated for each position x within the volume of the plank by integrating over the surface of the cross-sectional area of the plank (Eq. 9).

$$E_{a,BT}(x) = \frac{\iint E_x dydz}{b \times h} \quad (9)$$

The apparent axial MoE can be calculated as the harmonic mean of the localized MoE, i.e., the equivalent stiffness of series springs of individual stiffness $E_{a,BT}(x)$ (Eq. 9) averaged over a length of 90 mm (Olsson et al. 2019) (Eq. 10). This variable is the IP of the tensile strength that will be used in the present study.

$$E_{a,app,90,BT}(x) = 90 / \int_{x-\frac{90}{2}}^{x+\frac{90}{2}} \frac{1}{E_{a,BT}(\xi)}\, d\xi \tag{10}$$

where app stands for apparent, BT refers to analytical beam theory and $d\xi = 1$ mm by numerical integration.

Sampling and digitalization

Two different samplings were used for the present study. The first one is constituted of 924 oak planks that were carefully selected following the guidelines of EN 14081-2 (2022), focusing on a specific quality representative of the resource that would be used in a sawmill to produce structural timber. This sampling was aimed to assess the mechanical modelling used to predict the tensile strength, which is explained in detail in (Pot et al. 2024).

The second sampling is specifically designed for this present study. It is constituted of 92 dry oak boards. They were coming from the same batch as the previous one, but with a single cross-section measuring 21 × 70 mm². The strategic objective is to use narrow width timber, which has lower economic cost, for the manufacture of glued timber such as finger-jointed lamellas. An industrial scanner (X-Scan, Luxscan), was used to analyze the boards in depth. By moving the boards longitudinally, the scanner provides detailed images of all four long faces, while capturing crucial data such as local density and fiber orientation. Fiber orientation data was obtained by detecting and processing laser points. Each face of the boards was subjected to a laser spot projected perpendicular to the surface, scattered into multiple laser spots via a diffractive optical element. The local orientation of the fibers is defined by the angle of the major axis of the ellipse, and these measurements over the entire surfaces (out of the front and end faces) of the boards were used to construct detailed maps. These maps were used for the visual representation of the data (Figure 2), and the MoE profile calculation along the board as described above.

Figure 2: Visualisation of the distribution of angles on the 4 faces of a board. The profile shown is the average over 90 mm with an average standard deviation.

Optimization of the boards cross-cutting for finger-jointing

Calculation of the tensile strength thresholds for lumber

This study focuses on developing a method ensuring the mechanical strength of finger-jointed lamellas corresponding to a single class. It was chosen to test the method for a tensile strength class T11 of (NF EN 338 2016) standard. This implies a strength of 11 MPa for clear wood and 16 MPa for the finger-joints (NF EN 14080 2013). The IP thresholds corresponding to these requirements were defined as follows.

As explained in (Pot et al. 2024) for each of the 924 boards, the minimum value of $E_{a,app,90,BT}(x)$ along the profile was used as the IP representing the board tensile strength, which lead to the scatter plot of figure 3. For every possible IP threshold, the characteristic tensile strength of the boards whose IP values

are higher than that threshold was calculated following (NF EN 14358 2016). The IP threshold value is the IP corresponding to the characteristic strength target (T11 class in this case). A similar analogy was made for finger-joints, following the strength condition recommended in the standard (NF EN 338 2016). The selected tensile class corresponds to thresholds of 6.55×10^3 MPa to ensure a wood tensile strength of 11 MPa (corresponding to the T11 class), and 9.23×10^3 MPa to ensure a finger-joint strength of 16 MPa (NF EN 14080 2013). They are shown in Figure 3.

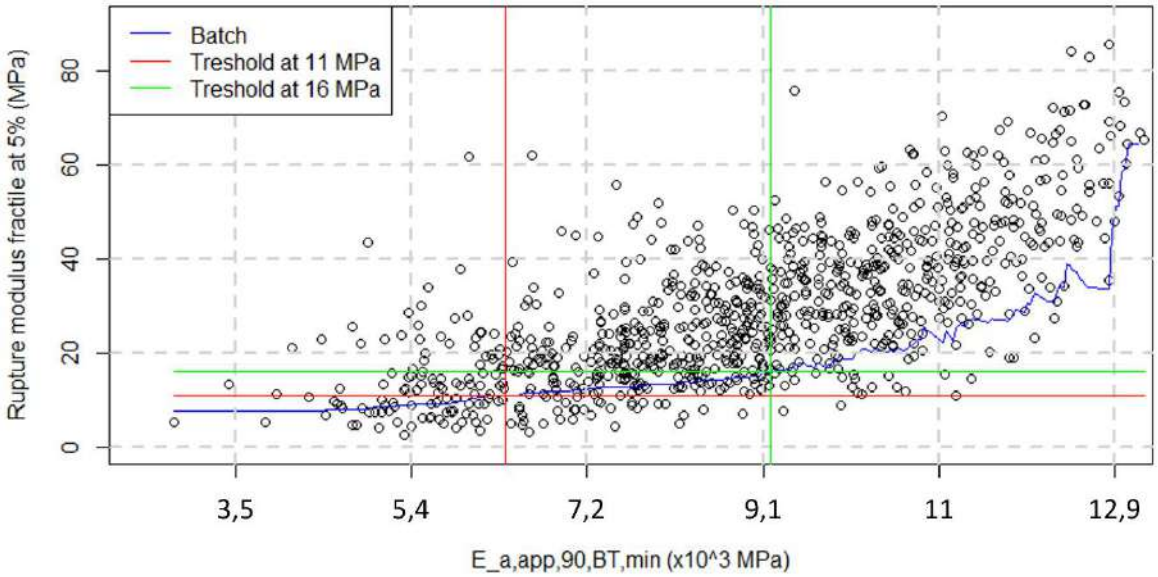

Figure 3: Tensile modulus of rupture thresholds determination

Digital twin for the cross cutting optimized localization

A numerical algorithm was developed to simulate the cross-cutting operation. The code is based on the stiffness profiles (Figure 4) to perform the cross-cutting in two distinct steps. The first step is to exclude areas of the board where the IP is below the threshold ensuring the wood strength of 11 MPa, while ensuring that the remaining pieces have a minimum IP at the ends ensuring the 16 MPa for finger-jointing.

The second step relates to the dimensions of the remaining pieces. The industrial finger-jointing line which was used imposes constraints on the length of the finger-jointed pieces, stipulating that they cannot be shorter than 250 mm or longer than 900 mm. So, the process consists of going through the profile in the sections to be kept. For each remaining piece longer than 900 mm, the cut is made at the 900 mm position, if the part at this position has a modulus at least equal to the finger-jointing threshold and that the rest of the piece is at least 250 mm long. If the remaining piece is less than 250 mm long, the 900 mm position is shifted backwards until the remaining wood is at least 250 mm long. In all cases, it is essential to ensure that the boards to be preserved are between 250 mm and 900 mm long, and that the cut-off positions have IP compatible with the required finger-joint strength. Figure 4 shows the cut-off positions as dotter red lines. In total, 236 cross cuts were performed from the 92 boards.

	Axial tensile strength (MPa)	Characteristic resistance (MPa)	Elastic modulus threshold (MPa)
Wood	$f_{t,0,k}$	11	6.55×10^3
Finger-joint	$f_{t,j,k}$	16	9.23×10^3

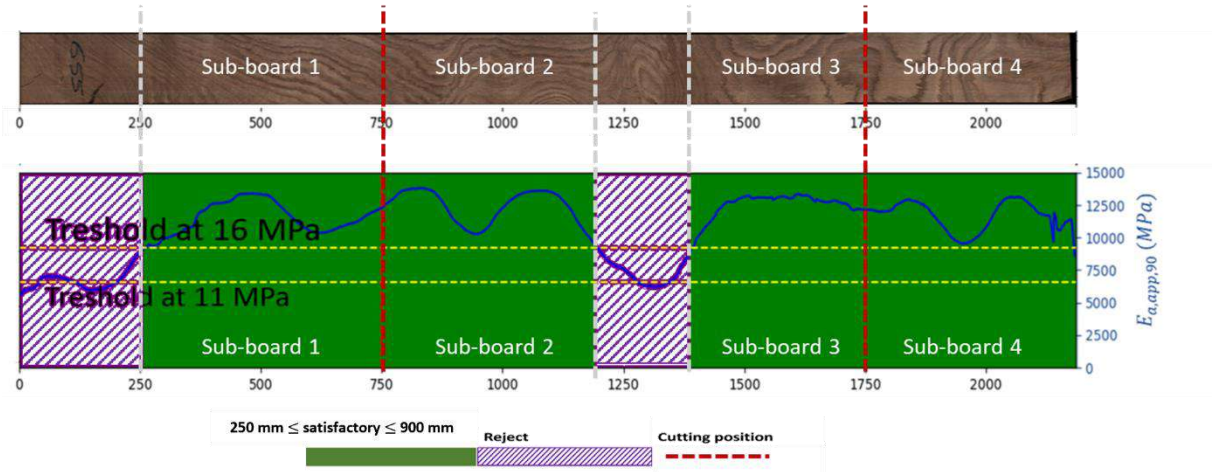

Figure 4: Example of the cross-cutting optimization algorithm application. In purple the removed parts, and in green the kept ones.

A total of 79 finger-jointed lamellas of varying lengths, with a cross-section of 21 × 70 mm² were produced, cut into 183 small finger-jointed strips in order to test as many finger-joints as possible, while complying with the recommendations of the standard (NF EN 408+A1 2012). Figure 5 shows an example of a finger-jointed lamella made from the pieces of wood produced by cross-cutting. During finger-jointing, the ends of the boards are trimmed by 7 mm, and 10 mm long teeth are machined, with a pitch of 3.8 mm. These additional reduction were not anticipated during the cutting process, but the cut positions obtained ensure that the boards can be finger-jointed for at least 17 mm in the direction of reduction.

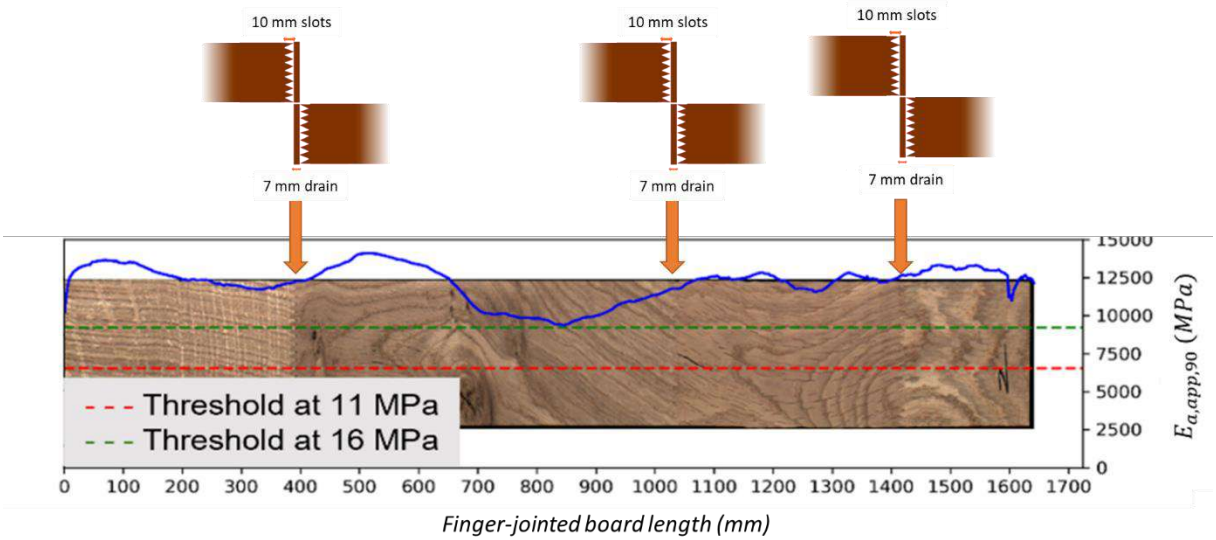

Figure 5: Example of a manufactured finger-jointed board glued with polyurethane (PU)

Tensile tests were carried out on the finger-jointed lamellas in accordance with (NF EN 408+A1 2012). Figure 6 shows the test conditions. Joint shall be located at the center span and the test length clear of machine grips is at least nine times the smallest cross-sectional dimension. The tensile strength ($f_{t,0}$) is given as function of the maximum load (F_{max}) and the cross-sectional area (A) by the following Eq. 7:

$$f_{t,0} = \frac{F_{max}}{A} \quad (7)$$

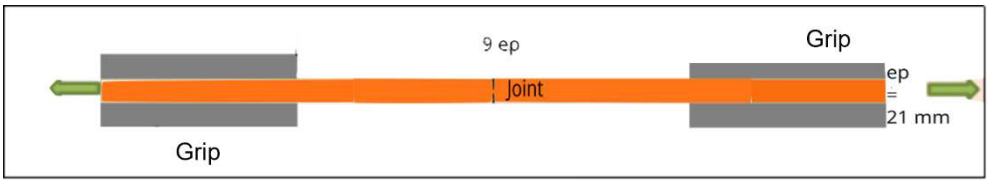

Figure 6: Tensile test

RESULTS AND DISCUSSIONS

Experimental strength of finger joints

Figure 7 shows the strength distribution obtained from finger-joints tensile tests. The average tensile strength for the full series is 28.69 MPa corresponding to a characteristic strength of 18.33 MPa.
However, two failure types can be distinguished. The test results were classified into two groups according to whether the lamella broke in the finger-joint or elsewhere in the wood other than in the finger-joint (see examples of failure types in Figure 7). The results are presented in Table 3. The failure rate of lamellae in finger-joints was 31%, whereas outside the finger-joints, it was 69 %. The corresponding characteristic strength were 20.41 MPa and 17.32 MPa, respectively. This behaviour was expected, because the full cross-cutting process was designed to ensure a wood tensile strength above $f_{t,0,k}$, which is 5 MPa lower than $f_{t,j,k}$. As a result, the chance of having a strength of the lamella within the 9 times *h* distance below $f_{t,j,k}$ is rather high, and finger-joints often exhibit a greater strength than the wood around it.

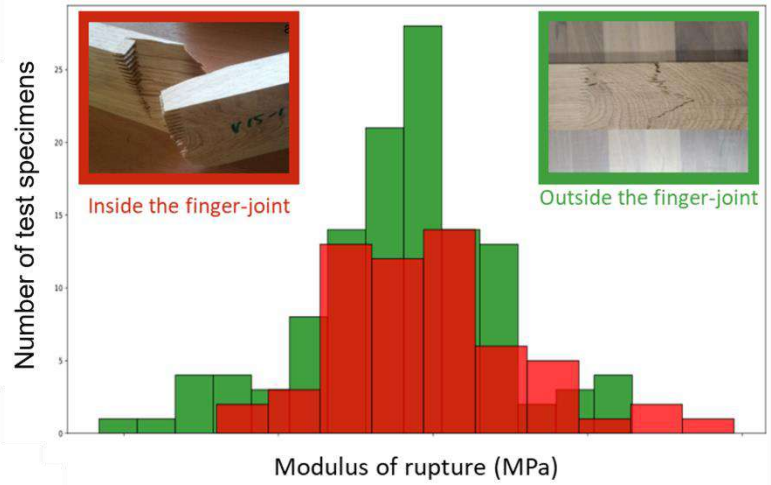

Figure 7: Histogram distribution of strength obtained from tensile tests: failure outside of the finger-joints (green); failure in the finger-joints (red) together with their post-failure figure

Table 3: Results of finger-joints tensile tests.

Failure zone	Percentage	Characteristic strength
All	100%	18.33 MPa
Outside of the finger-joints	69%	17.32 MPa
In the finger-joints	31%	20.41MPa

The characteristic finger-joints tensile strength corresponds to the case when the failure occurs inside the finger-joints. The minimum value observed in this case is 15.99 MPa, which is sensibly equal to (even slightly higher than) the T11 class threshold. The absence of low-strength finger-joints could be due to the fact that the targeted class is low and thus the 16 MPa threshold is easy to reach. It is also important to remember that the profiles are averaged over a length of 90 mm centered, which can affect the precision of the cut positions and explain this behaviour.

Prediction of finger joint strength using image reconstruction and elastic modulus profiles

A Python code has been developed to reconstruct numerically the finger-joints. The code takes as input the positions and profiles of the finger-joints in the initial boards (boards before cutting), and assembles them exactly as it was done physically (Figure 8). The strength of the finger-joint is predicted as the minimum value between the average profile value in the left finger-joint (length of 10 mm) and the average profile value in the right finger-joint (length of 10 m) as finger-joints machining described in Figure 5.

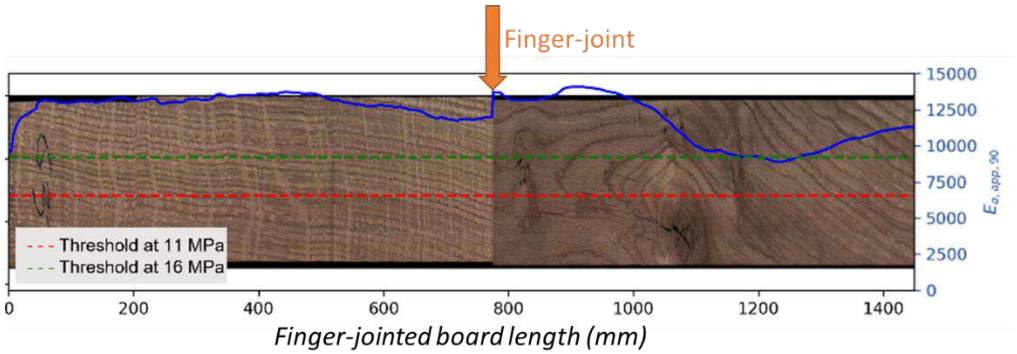

Figure 8: Example of a reconstructed finger-joint (in blue, $E_{a,app,90,BT}$)

The characteristic value of the finger-joint strengths predicted by image and profile reconstruction is 16.45 MPa, which satisfies the previously recommended joint strength condition.

Figure 9 illustrates the distribution between experimental and predicted strengths, along with the density in the finger-joints (averaged as above). The dispersion of points in the scatter plot could be attributed to the fact that the profile obtained by image reconstruction behaves as if the finger-joint assembly was perfect without discontinuity, while actually there is an effect of finger-joint and the strength of the adhesive used, which increases the strength within the finger-joints. Density may explain for some points that a predicted value may be low, for example (as the prediction is primarily based on fiber orientation), but high in reality due to its high density, and vice versa.

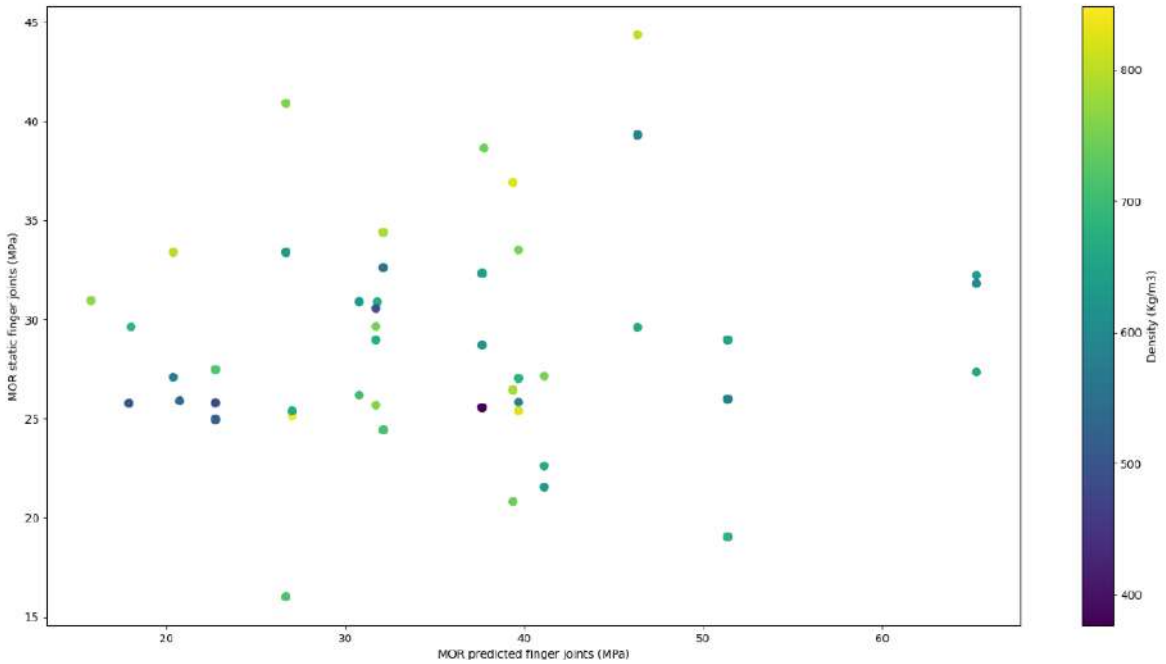

Figure 9: Correlation between tensile strengths (experimental and predicted) with their density

CONCLUSION

These findings represent another step forward, proposing an optimization method to cross-cut boards for finger-joints engineered wood products (CLT, GLT) based on surface fiber orientation scanning of the sawn boards. Since scans of the boards provide surface information, a very important phase is the interpolation within the volume and the mechanical global modelling of the board. The results show that the proposed method effectively ensures lamellas of T11 class. However, the measured finger-joints characteristic tensile strength was higher than expected, suggesting that it could be improved to reduce material waste. A verification of the method could be made by applying it similarly for another class greater than T11 (T14 for example). Although the finger-joints strength prediction based on fiber orientation seems working, it's important to quantify the material yield because that's what will generate the added value in industrial context, thus, future works will focus on this matter.

ACKNOWLEDGEMENTS

This work was supported by the French Environment and Energy Management Agency (ADEME).

REFERENCES

Besseau B (2021) Contribution au développement de procédés innovants pour une transformation plus efficiente du chêne. These de doctorat, HESAM

Daval V, Pot G, Belkacemi M, Meriaudeau F, Collet R (2015) Automatic measurement of wood fiber orientation and knot detection using an optical system based on heating conduction. Opt Express 23(26):33529–33539. https://doi.org/10.1364/OE.23.033529

EAD 130320-00-0304 (2018) Glued laminated timber made of solid hardwood

EN 14081-2+A1 (2022) Timber structures - Strength graded structural timber with rectangular cross section - Part 2: Machine grading; additional requirements for type testing

Kretschmann DE (2010) Wood handbook, chapter 05: mechanical properties of wood. For. Prod. Lab. Dep. Agric. For. Serv. Madison Wis. USA

NF EN 338 (2016) Structural timber - Strength classes

NF EN 408+A1 (2012) Timber structures - Structural timber and glued laminated timber - Determination of some physical and mechanical properties

NF EN 14080 (2013) Timber structures - Glued laminated timber and glued solid timber - Requirements. https://cobaz-afnor-org.rp1.ensam.eu/notice/norme/nf-en-14080/FA170492?rechercheID=2213043&searchIndex=1&activeTab=all#id_lang_1_descripteur. Accessed 21 Jul 2021

NF EN 14358 (2016) Timber structures - Calculation and verification of characteristic values

Nyström J (2003) Automatic measurement of fiber orientation in softwoods by using the tracheid effect. Comput Electron Agric 41(1–3):91–99. https://doi.org/10.1016/S0168-1699(03)00045-0

Olsson A, Briggert A, Oscarsson J (2019) Increased yield of finger jointed structural timber by accounting for grain orientation utilizing the tracheid effect. Eur J Wood Wood Prod 77(6):1063–1077. https://doi.org/10.1007/s00107-019-01465-0

Pot G, Viguier J, Besseau B, Lanvin J-D, Reuling D (2024) Modelling tensile mechanical properties of oak timber from fibre orientation scanning for strength grading purpose. Sopron, Hungary

Purba CYC, Viguier J, Denaud L, Marcon B (2020) Contactless moisture content measurement on green veneer based on laser light scattering patterns. Wood Sci Technol 54:891–906. https://doi.org/10.1007/s00226-020-01187-0

Simonaho S-P, Palviainen J, Tolonen Y, Silvennoinen R (2002) Determination of wood grain direction from laser light scattering pattern. Opt Lasers Eng 41(1):95–103. https://doi.org/10.1016/S0143-8166(02)00144-6

Simonaho S-P, Silvennoinen R (2004) Light Diffraction from Wood Tissue. Opt Rev 11(5):308–311. https://doi.org/10.1007/s10043-004-0308-8